Selective Hydrogenation of Acetylene in an Ethylene Rich Flow: Results of Kinetic Simulations

Jason Gislason, Wensheng Xia, and Harrell Sellers*

Department of Chemistry and Biochemistry, South Dakota State University, Brookings, South Dakota 57007

Received: April 2, 2001; In Final Form: October 18, 2001

We have performed kinetic simulations of the behavior of acetylene hydrogenation under ethylene rich conditions at a number of temperatures and feed gas compositions employing Pd and Pd/Ag alloy catalysts. The results of these simulations form a clear and consistent picture as to the origins of selectivity, thermal runaway, oligomer formation, the role of CO as a promoter of selectivity and inhibitor of oligomer formation, and the importance of proton transfer among carbonaceous species. The modeling gives insight into mechanistic details and provides an explanation for the influence of alloying catalyst on these phenomena.

Introduction

Ethylene is important as a raw material for polyethylene production, which is often produced by the thermal or catalytic cracking of saturated or higher hydrocarbons.[1] The product stream of the cracking process consists of a mixture of saturated and unsaturated hydrocarbons, hydrogen, and carbon monoxide, the composition of which is dependent on the feedstock and operating conditions of the cracking process.[1] A typical composition of a cracked hydrocarbon stream is shown in Table 1. Before the cracked hydrocarbon stream can be used as the feedstock for the ethylene polymerization reactor, the concentration of acetylene in the feedstock must be decreased below 5 ppm[2] because acetylene stoichiometrically poisons the ethylene polymerization catalyst.[3]

The selective hydrogenation of acetylene in the ethylene rich flow is the primary method of reducing the acetylene concentration. In this process, acetylene is hydrogenated without significant hydrogenation of ethylene over a supported metallic catalyst in an adiabatic, packed-bed reactor.[2] Palladium catalysts are the most selective unimetallic catalysts for this acetylene hydrogenation process.[2] The acetylene removal units (ARUs) are operated either as "tail-end" or "front-end" reactors. The tail-end reactor feedstock is fractionated before the hydrogenation process,[1] which removes the majority of the carbon monoxide and hydrogen from the flow. Tail-end ARUs operate at a hydrogen concentration just greater than the acetylene concentration. Front-end reactors receive an unfractionated feedstock directly from the cracker,[1] which is rich in hydrogen and often contains a small fraction of carbon monoxide.

The mechanism for selective hydrogenation of acetylene in an ethylene rich flow over palladium and palladium alloy catalysts has been extensively studied.[1−59] Previous kinetic studies yielded inconsistent results, leading to the proposal of one,[41,60] two,[3,53,61] and even three[18−20] types of active sites on the catalyst. Each site has been attributed with different hydrogenation properties to explain the selectivity of the catalyst. Hydrogen atoms, molecular hydrogen, subsurface hydrogen,[27,62] and adsorbed carbonaceous[4,5] species have each been proposed as possible primary hydrogen sources. Recently, Tysoe et al. indicated that the rate-limiting step for the $C_2H_2 + H_2$ reaction should happen before the hydrogenation of vinyl radical.[63] They reported[64] that the activation barrier on Pd surface was 9.6 ± 0.2 kcal/mol at 300 K and 100 torr H_2 pressure.

TABLE 1: Typical ARU Feedstock Composition

species	concentration
methane	10%
ethane	25%
hydrogen	25%
ethylene	39%
acetylene	0.4%
carbon monoxide	250 ppm

We have applied recently developed techniques for the modeling of heterogeneous catalysis to study the selective hydrogenation of acetylene on Pd and Pd/Ag alloy catalysts. In this work we calculated the Arrhenius reaction rate constants and solved the rate equations for a large set of reactions. This is one of the first times that rate constants from purely theoretical methods have been successfully employed in a *large* set of elementary reactions for the description of an industrial process. The solutions we obtained give new insight into the reaction mechanism with changing temperature, pressure, feed gas, and catalyst composition. Herein we discuss the results we obtained from our kinetic modeling and their implications regarding the mechanism of selective hydrogenation over Pd and Pd/Ag alloy catalysts.

Modeling Details

Methods used in this work to obtain Arrhenius rate constants for elementary reactions are published elsewhere.[65−74] Herein we briefly sketch the process, since these methods are not in widespread use.

Kinetic Simulations. We solved the kinetic equations defined by a set of coverage dependent Arrhenius reaction rate constants for a moderately large set of reactions (see Table 2) which included (a) adsorption and desorption of H_2, acetylene, ethylene, methane, ethane, and CO; (b) displacement reactions in which gas-phase components displace surface phase components, the most important of which are the displacement of H_2, acetylene, ethylene, methane, and ethane by gas-phase CO

* Corresponding author. E-mail: harrellsellers@hotmail.com.

10.1021/jp011238s CCC: $22.00
Published on Web 01/11/2002

TABLE 2: Reactions Defining the Kinetic Mechanism Employed in This Work

process	species/reaction
adsorption/desorption	H_2, C_2H_2, C_2H_4, C_2H_6[a], CO[b], green oil[a]
single hydrogen addition:	$H + C_2H_n \rightarrow C_2H_{n+1}$, $n = 1-5$
	$H + C_4H_n \rightarrow C_4H_{n+1}$, $n = 6-9$
single hydrogen addition:	$H_2 + C_2H_n \rightarrow C_2H_{n+1} + H$, $n = 1-5$
	$H_2 + C_4H_n \rightarrow C_4H_{n+1} + H$, $n = 6-9$
C−H dissociation:	$C_2H_n \rightarrow C_2H_{n-1} + H$, $n = 2-6$
H−H dissociation/recombination	
displacement reactions[c]	
gas-phase CO displacing surface phase:	
H_2, C_2H_2, C_2H_4, C_2H_6	
oligomerization reactions[d]	vinyl + $C_2H_n \rightarrow C_4H_{n+3}$, $n = 2-5$
	ethyl + $C_2H_n \rightarrow C_4H_{n+5}$, $n = 2, 4$

[a] Only desorption was considered. In the case of ethane, it was not present in the feed gas. [b] Kinetics simulations were performed with and without CO in order to understand the role of the coadsorbate. [c] Many other displacement reactions were originally present in the mechanism and found to be unimportant. A detailed description of our treatment of displacements has been submitted for publication. [d] All the oligomerization reactions are diffusion controlled and their rate constants are similar.

and vice versa; (c) H_2 dissociation and recombination; (d) H_2 + acetylene, ethylene, vinyl, C_2H_5, and C_4 radicals; (e) H + acetylene, ethylene, vinyl, C_2H_5, and C_4 radicals; (f) oligomerization reactions: vinyl + vinyl, vinyl + acetylene, vinyl + ethylene, C_2H_5 + vinyl, acetylene, ethylene, and C_2H_5 + acetylene, ethylene. The apparent activation barrier for an elementary reaction is bound by the intrinsic activation and diffusion barriers[73] (by "intrinsic" we mean the activation barrier without a diffusion contribution). We employed intrinsic activation barriers in this work for reactions that are not diffusion-controlled. Diffusion barriers were taken to be the activation barriers of diffusion-controlled reactions (small or no intrinsic barrier). This reaction set defines the kinetic mechanism employed in this work and can be used to reproduce our results. Coverage effects in the kinetic simulations were taken into account according to the UBI-QEP method.[73] This should not be confused with the coadsorbate coverage of 0.4 that we use for discussion purposes in Table 3. In the kinetic simulations it was not necessary to consider the effect on heats of adsorption of more than one coadsorbate because of the relative coverages.

The set of differential equations resulting from this mechanism and our rate constants is extremely stiff, particularly in the beginning of the calculation. When beginning with a clean surface, the time step had to be small ($\sim 10^{-14}$ to 10^{-15} seconds) in order for the set of equations to be stable (stable means the solution does not diverge or blow up). On a 450 MHz computer, a kinetic simulation, beginning with a clean surface, may take a week or longer to reach a "steady operating state" in which the surface coverages are relatively constant in time. As the surface coverages approach constancy, the time step can be increased. Then it may take 12 h of computer time to simulate a microsecond of kinetics for some mechanisms. This might be drastically reduced by running the simulations on a parallel computing system.

Relevance of the Kinetic Model to Industrial Conditions. Industrial acetylene hydrogenation reactors are adiabatic, packed-bed reactors.[2] Certainly our kinetic simulations do not account for all aspects of commercial industrial reactors. We have not incorporated any fluid dynamics, nor have we modeled any heat transfer phenomena. There is no explicit flow rate of the feed gas per se in our kinetic model. Each of our kinetic simulations was performed at a selected, constant temperature (isothermal), and the products that desorb from the metal surface are "swept away" so that the composition of the feed gas in contact with the surface does not change. Feed gas of a specific composition, temperature, and pressure is in contact with the catalyst, the products form and move away from the particular section of catalyst surface under study. This most nearly approximates a cross-sectional slice through the packed-bed reactor (plug flow), which has associated with it a specific feed gas composition and temperature (for example, from a measured temperature profile). The conditions under which we solved the kinetics are defined in Table 1 with a total pressure of 500 psi. We solved the kinetics equations with and without CO and for Pd and Pd/Ag alloy catalysts. Although activation barriers corresponding to the fcc(111) surface were employed in the simulations reported herein, we have performed numerical experiments with other low-index, thermodynamically stable surfaces and obtained similar results.

Below we make statements regarding the phenomenon of thermal runaway. It may seem at first that this is not possible from results of isothermal kinetic simulations. However, thermal runaway is associated with excess ethane production. We argue that the temperature at which ethane production increases rapidly correlates with the onset of thermal runaway. This temperature can be identified from a set of (isothermal) kinetic simulations performed at different temperatures in which ethane production is determined.

Rate Constant Determination. We determined the rate constants from several new theoretical procedures. We employed our Normalized Bond Index Reactive Potential Functions (NBI−RPF)[65−70] in molecular dynamics (MD) simulations of reactions on the catalyst surface using activation barriers obtained from the Unity Bond Index-Quadratic Exponential Potential (UBI-QEP) method of Shustorovich and Sellers.[73] Together the UBI-QEP method, yielding activation barriers, and the MD simulations, yielding Arrhenius preexponential factors, define a specific rate constant. We often employed a statistical mechanical approach[74b] to calculate the ratio of preexponential factors for forward and reverse reactions to avoid the computational burden of having to do MD simulations of slow processes. The calculated rate constants then define the parameters for a set of differential equations that we solved numerically. In the kinetic expressions, we included the empty surface binding sites needed for the products as reactants. The solutions give the coverage and product distribution as functions of time, temperature,

TABLE 3: Reactions and Intrinsic Activation Barriers[a] (kcal/mol) for Selected Important Reactions

	ΔE^*	
reaction	Pd	Pd/Ag
1. $H_2 \rightarrow H + H$	12	14
2. $H + C_2H_2 \rightarrow$ vinyl	0	0
3. $H + C_2H_4 \rightarrow$ ethyl	<2	1
4. $H_2 + C_2H_2 \rightarrow$ vinyl + H	2	4
5. $H_2 + C_2H_4 \rightarrow$ ethyl + H	7	9
6. H + vinyl $\rightarrow$ ethylene	8	5
7. H + ethyl $\rightarrow$ ethane	0	0
8. H_2 + vinyl $\rightarrow$ ethylene + H	0	0
9. H_2 + ethyl $\rightarrow$ ethane + H	0	0
10. C_2H_2 desorption	13	11
11. C_2H_4 desorption	11	10
12. CO desorption	25	24
13. H_2 desorption	6	5
14. oligomerization: all C_2 radicals + $C_2 \rightarrow C_4$	0	0

[a] For the cases in which the intrinsic activation barriers are zero or low, the diffusion barriers[73] were employed in the simulations as the reaction activation barriers.

pressure, and composition of the feed gas and catalyst. The rate constants we determined in this work are available as part of the Brookings Kinetics Database maintained by Chemical Process Modeling, Inc.[75]

Results

We focus the discussion of the mechanism of selective hydrogenation on a subset of the reaction set used in the simulations. A small reaction set is given in Table 3 along with the activation barriers for Pd and Pd/Ag alloy catalysts. For the purposes of this discussion the values in Table 3 are relevant to a coadsorbate coverage of 0.4, which has a heat of adsorption of 25 kcal/mol. Displaying activation barriers this way (at an arbitrary coverage with a reasonable but fictitious coadsorbate) allows us to incorporate some coverage effects in a general and average way for discussion purposes without having to make the discussion relevant to a specific point in any one kinetic simulation. In the actual simulations, the coverage effects were incorporated in a more rigorous way. These data account for the selectivity of the catalyst and the increase in selectivity upon alloying with silver and, together with the results of the kinetic simulations, explain the role of CO and the underlying causes of thermal runaway.

The accuracy of the activation barriers determined with the UBI-QEP method is actually not that easy to assess. Certainly, at some point the level of accuracy of the barriers is a limitation of the method, and in that respect, our work here is a test of the applicability of these methods to the modeling of kinetics. The UBI-QEP barriers usually agree with experimental values to within 1−3 kcal/mol. There are inaccuracies in the experimental values as well, since they are usually obtained from fits to observed data with assumed Arrhenius preexponentials. Experimentally, preexponential factors often have uncertainties spanning 4 orders of magnitude.[74a] This range of preexponential, when applied to the fitting procedure for the determination of the dissociation rate constant of CN, gives an uncertainty of more than 9 kcal/mol (20%) in the zero coverage limit dissociation barrier.[74a] When the difference between a theoretical (UBI-QEP) barrier and an experimental one is 1 or 2 kcal/mol, it is not necessarily always clear that the experimental value is the better one. The quality of the kinetic description from modeling efforts such as these should be judged from the

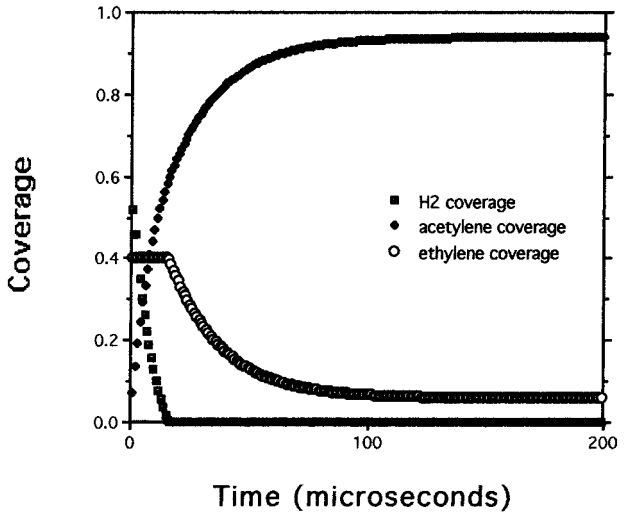

Figure 1. Competetive adsorption: coverages as a function of time of H_2, acetylene, and ethylene beginning from a clean Pd surface. To isolate adsorption/desorption processes, reactions among components were disallowed.

modeling results. From our results presented herein, it is evident that our rate constants are in the correct proportions.

Hydrogenation Mechanism. The selectivity for the hydrogenation of acetylene in an ethylene rich flow has been attributed to the greater heat of adsorption of acetylene than ethylene on the catalyst surface, because a small difference in the heats of adsorption of two molecules competing for the same binding site can cause a significant difference in their surface coverages.[76] The greater heat of adsorption of acetylene was believed to cause the catalyst surface to be predominately covered with acetylene.[17−20] Our kinetic simulations do not support this conclusion under the conditions employed in this work. The modeling indicates that, under these conditions, the selectivity is due to a number of influences and that the surface never has a very high coverage of acetylene.

Figure 1 shows the resultant coverages on Pd(111) of acetylene, ethylene, and hydrogen from a simulation of competitive adsorption, *in the physically unrealistic situation in which no reactions were allowed to take place between the reactants*. The purpose of this simulation was to show that consideration of heats of adsorption (adsorption/desorption processes) alone will give a false picture of what is on the surface. The feed gas is about 75 mole percent ethylene, 24.7 mole percent molecular hydrogen, and 0.3 mole percent acetylene. This kinetic simulation indicates that acetylene covers approximately 94% of the surface while the more weakly bound ethylene and hydrogen cover approximately 6% of the surface. This would seem to support the mechanism given above. However, when reactions among the adsorbates are included in the kinetic model, the surface coverage of acetylene drops to below 10^{-3} (depending on the parameter set used in the simulation). This drop in coverage is caused by the high reactivity of acetylene with atomic and molecular hydrogen to form vinyl radicals. This illustrates the importance of kinetic effects, specifically that kinetic effects can completely change the microscopic picture.

Origins of Selectivity. The mechanism for the selective hydrogenation of acetylene is a competition between a number of chemical processes. Table 3 contains the intrinsic activation barriers for selected important processes on the Pd and Pd/Ag alloy surfaces. We have made the point that it is dangerous to think in terms of activation barriers only. However, the barriers given below support the argument we present for the origins of

selectivity, and we agree that this is an imperfect argument lacking the kinetic effects.

The two main paths for the first hydrogen addition are:

$$\text{Path 1: } H_2 + C_2H_2 \rightarrow C_2H_3 + H \quad \Delta E^* = 2/4$$

$$H_2 + C_2H_4 \rightarrow C_2H_5 + H \quad \Delta E^* = 7/9$$

and

$$\text{Path 2: } H_2 \rightarrow H + H \quad \Delta E^* = 12/14$$

$$H + C_2H_2 \rightarrow C_2H_3 \quad \Delta E^* = 0/0$$

$$H + C_2H_4 \rightarrow C_2H_5 \quad \Delta E^* = <2/1$$

where the activation barriers are in kcal/mol and correspond to pure Pd and the Pd/Ag alloy for an average coverage of 0.4. Of the two paths, path 1 is clearly the more selective for acetylene hydrogenation. Maximum selectivity is obtained when path 2 is suppressed by the presence of CO and by alloying the Pd with silver.

Acetylene hydrogenation via path 1 is favored by the kinetics over path 2 and ethylene hydrogenation along path 1. For the hydrogenation of acetylene along path 1, the reaction barrier is lower than the desorption barriers of the reactants. This is not true for ethylene hydrogenation along path 1 or hydrogenation along path 2. Therefore, path 2 and ethylene hydrogenation along path 1 will be hindered by competing desorptions. The full kinetic simulation, which contains both atomic and molecular hydrogen, indicates that, *at higher coverages*, molecular hydrogen is the primary hydrogen source for the first hydrogen addition reaction, although atomic hydrogen contributes. We observed that putting the rate constant for H_2 reaction with acetylene and ethylene to zero caused a significant loss of selectivity and decreased the rate of consumption of acetylene.

On pure palladium the desorption of ethylene contributes to the selectivity. The desorption barrier of ethylene (Table 3) is only 4 kcal/mol more than the barrier for first hydrogen addition with H_2 as the hydrogen source. For acetylene, the desorption barrier is 11 kcal/mol greater. The modeling predicts that the increase in selectivity observed upon alloying Pd with Ag is due to (a) the shift in the hydrogenation barrier for ethylene even closer to the desorption barrier so that more ethylene desorbes rather than hydrogenates and (b) slowing of the dissociation rate of H_2.

We emphasize that the overall coverage influences the reaction mechanism of C_2H_2 hydrogenation, namely that at low overall coverages the primary hydrogen source is atomic hydrogen while at higher overall coverages molecular hydrogen is the dominant hydrogen source. Certainly hydrogenation by both atomic and molecular hydrogen contributes to the overall reaction mechanism. However, our modeling indicates that molecular hydrogen as the "dominant" hydrogen source is favored at relatively high overall coverages and maximum selectivity is achieved when the first hydrogenation by atomic hyrdrogen is suppressed. We argue that this makes sense just from the standpoint that atomic hydrogen is so mobile and reactive that significant selectivity for acetylene hydrogenation is not really possible if atomic hydrogen is the dominant hydrogen source for the full range of coverages. But, our kinetic model supports this contention by indicating that the rate of atomic hydrogen production is relatively low at higher overall coverages (where industrial hydrogenation reactors operate), due in large part to the relatively high H_2 dissociation barrier and the inability of molecular hydrogen to compete with other adsorbates for surface binding sites so that its presence on the surface is low.

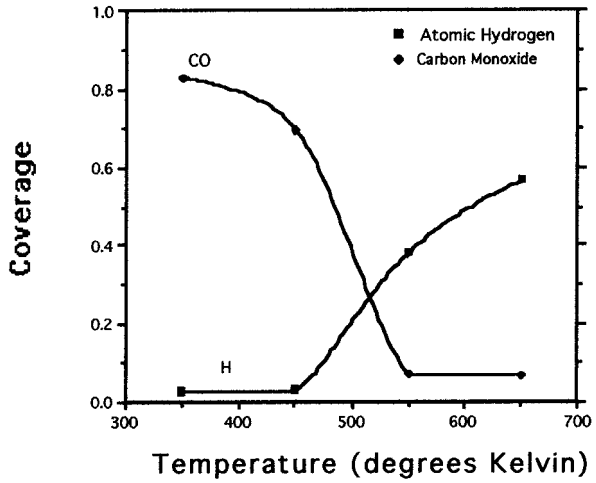

Figure 2. Steady state coverages of atomic hydrogen and CO on Pd/Ag alloy catalyst as a function of temperature.

Even though our kinetic simulations were performed under different conditions some of our results agree well with the conclusions of Azad et al.[63] Our modeling indicates that, under higher overall coverage conditions, which favor molecular hydrogen as the dominant hydrogen source, (1) hydrogenation of vinyl (via reaction with H_2) is more rapid than hydrogenation of acetylene (via reaction with H_2) and (2) that the rate-limiting step in the hydrogenation is the first hydrogen addition to acetylene. Azad et al.[63] came to the same conclusions.

Molero et al.[64] obtained a value of 9.6 kcal/mol for "acetylene hydrogenation" from experimental measurements. Their experiments were conducted at much lower pressures and temperatures than our simulations. We are not able to judge the overall coverage levels on their catalytic foils during their experiments; however, if their data correspond to relatively low coverages, then our modeling data would indicate that the atomic hydrogen path (path 2 above) is relevant to their work. Our modeling indicates (see Table 3) that, in path 2, the rate-limiting step is the dissociation of molecular hydrogen with a barrier of about 10−12 kcal/mol depending on coverage. This is in agreement with their data and their conclusion that the rate-limiting step comes before the hydrogenation of vinyl.

The influence of overall coverage on the reaction mechanism and selectivity is seen in the behavior of the system upon coadsorption of CO. Figure 2 is a plot of CO and H coverage as a function of temperature as obtained from our kinetic simulations of the Pd/Ag alloy catalyst. The atomic hydrogen coverage increases sharply at about 450 K and increases with temperature as the CO coverage falls. This is accompanied by a sharp increase in the ethane production (Figure 3), which signals the loss of selectivity. This effect is more dramatic on the pure Pd catalyst. Figure 4 shows the enhanced ability of the alloy catalyst to maintain a lower H coverage at higher temperatures.

Proton Transfer among Carbon Bearing Species. The self-hydrogenation of ethylene and acetylene has been shown to occur on metal surfaces.[18,19,31,32,35,37,77,78] We obtain the results that the activation barriers for self-hydrogenation are greater than the barriers for hydrogenation by H_2 by about 7 and 14 kcal/mol higher for ethylene and acetylene, respectively (Table 4). The hydrogenation of acetylene by ethylene can be expected to occur on the surface, because this hydrogenation barrier is

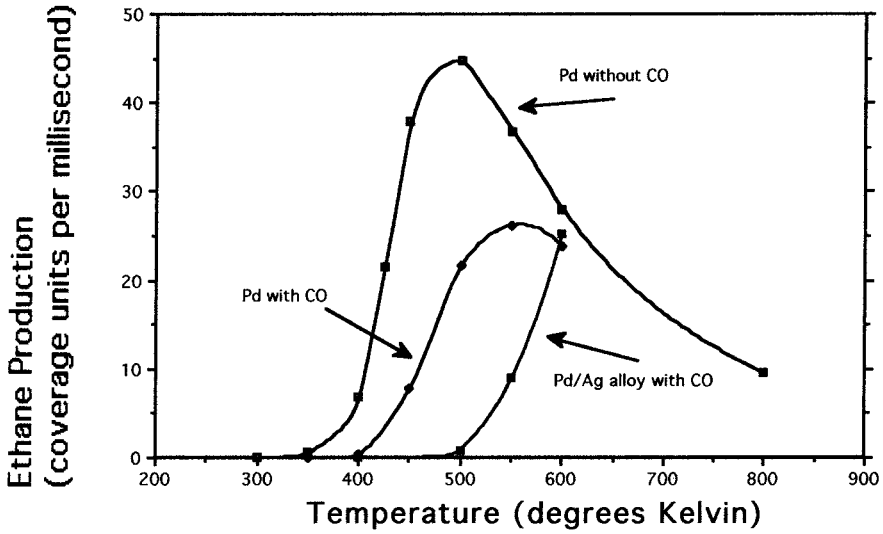

Figure 3. Rate of ethane evolution from catalyst surfaces as a function of temperature.

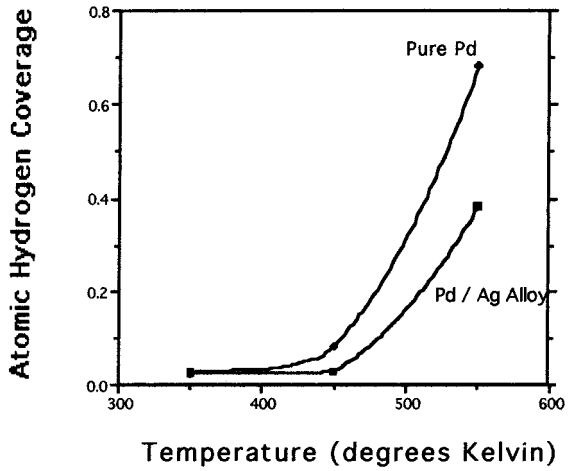

Figure 4. Atomic hydrogen coverage on Pd and Pd/Ag alloy catalyst as a function of temperature.

TABLE 4: Intrinsic Activation Barriers (kcal/mol) for Proton Transfer from Carbonaceous Species to Acetylene and Ethylene on the Pd/Ag Alloy[a]

reaction	ΔE^*
$C_2H_4 + C_2H_2 \rightarrow 2$ vinyl	9
$C_2H_4 + C_2H_2 \rightarrow CCH +$ ethyl	21
$2\ C_2H_4 \rightarrow$ ethyl + vinyl	14
$2\ C_2H_2 \rightarrow$ vinyl + CCH	17
$C_2H_2 +$ ethyl $\rightarrow$ vinyl + C_2H_4	0
$C_2H_2 +$ vinyl $\rightarrow$ vinyl + CCH_2	9
$C_2H_2 +$ ethyl $\rightarrow$ vinyl + $CHCH_3$	17
$C_2H_4 +$ ethyl $\rightarrow$ ethane + vinyl	2
$C_2H_4 +$ vinyl $\rightarrow CCH_2 +$ ethyl	14
$C_2H_2 + CHCH_3 \rightarrow$ vinyl + CCH_3	11
$C_2H_2 + CHCH_3 \rightarrow 2$ vinyl	0
$C_2H_2 + CCH_3 \rightarrow$ vinyl + CCH_2	0
$C_2H_2 + CCH_2 \rightarrow$ vinyl + CCH	22
$C_2H_4 + CHCH_3 \rightarrow$ ethyl + CCH_3	14
$C_2H_4 + CHCH_3 \rightarrow$ ethyl + vinyl	5
$C_2H_4 + CCH_3 \rightarrow$ ethyl + CCH_2	0
$C_2H_4 + CCH_2 \rightarrow$ ethyl + CCH	30
$C_2H_4 +$ ethane $\rightarrow 2$ ethyl	15
$C_2H_2 +$ ethane $\rightarrow$ vinyl + ethyl	10

[a] Activation barriers on pure Pd are similar.

around 9 kcal/mol. However, when H_2 is available, the modeling predicts that this reaction is not a significant contributor to acetylene hydrogenation because the barrier for acetylene hydrogenation by H_2 is 7 kcal/mol lower than this barrier. When this reaction does occur, there are two vinyl radicals in close proximity to one another on the palladium surface facilitating the formation of 1,3-butadiene (we do not mean to imply that this is a result of our simulations, since our kinetics are not spatially resolved finely enough to account for this effect). So, the hydrogenation of acetylene by ethylene most probably leads to the formation of C_4 compounds and heavier oligomers and not ethylene. The self-hydrogenation reactions are disproportionation reactions that have relatively small preexponential factors, which will further decrease the rate of reaction.

The proton transfer reactions from carbonaceous species to ethylene and acetylene have barriers comparable to or higher than those in the self-hydrogenation reactions except for the proton transfer from ethyl, ethylidene, and ethylidyne. The intrinsic hydrogenation barriers for ethylene and acetylene with ethyl, ethylidene, and ethylidyne as the hydrogen sources are small or zero so that the reactions are diffusion controlled (Table 4). For the proton transfer from ethylidyne, this is essentially the mechanism proposed Zaera and Somorjai where hydrogen is transferred from the surface bound carbonaceous layer to the reactants.[4,5] Experimentally, the formation of ethylidyne has been observed to be 2−3 orders of magnitude slower than the hydrogenation of ethylene.[13−15] Unlike experimental laboratory results not under normal ARU operating conditions,[4−8,10−15,20,27,29,30,41,79,80] our kinetic simulations employing industrial-like conditions showed that the surface coverage of ethylidene, vinylidene, and ethylidyne is insignificant. Therefore, some ethylene or acetylene hydrogenation due to hydrogen transfer from these radicals can occur, but the rate is slow enough that the effects on the overall mechanism are negligible. Proton transfer from ethyl to acetylene or ethylene is more probable judging from our simulations but is a minor contributor in the overall mechanism.

Oligomer Formation. The primary goal of the ARU is to hydrogenate acetylene to ethylene. However, it is well known that over 25% of the acetylene removed from the flow is lost to oligomer formation.[53] The reactions among C_2 radicals and between C_2 radicals and C_2 molecules have zero intrinsic activation barriers and are therefore diffusion controlled (Table 3). Therefore, the rate of oligomer formation is controlled by the competition of the diffusion controlled C_2 second hydrogenation and the diffusion controlled oligomer formation reactions. The UBI-QEP diffusion barrier for vinyl is about

7 kcal/mol, and our calculated diffusion barrier for molecular hydrogen is less than 1 kcal/mol.

The C_4 fraction of the oligomers formed on palladium has been reported to be composed largely of 1-butene, *trans*-2-butene, *cis*-2-butene, and *n*-butane.[3] One can envision elementary reactions that form these C_4 species. 1-Butene can be formed from the recombination of vinyl and ethyl radicals. However, the rate of this reaction would be low due to the low surface concentration of vinyl and ethyl radicals. 1-Butene can also be formed from the nonelementary, two-step reaction between vinyl and ethylene followed by hydrogen addition. *trans*-2-Butene and *cis*-2-butene can be formed from the recombination of ethylidene radicals or hydrogenation and rearrangement of 1,3-butadiene. However, the coverage of ethylidene radicals is low due to the slow formation of ethylidyne. The distribution of C_4 species observed during acetylene hydrogenation is similar to the distribution observed during 1,3-butadiene hydrogenation on palladium.[45−50] Similarly, it has been observed that C_4 species are derived primarily from acetylene.[16,28,38,39] These two observations indicate that C_4 formation could occur predominately by vinyl recombination, where the vinyl radicals are derived exclusively from acetylene under conditions in which ethylene coverage is low. Our simulations indicate that the formation of vinyl under these conditions comes predominately from acetylene. The activation barriers for dehydrogenation of ethylene to vinyl are mostly above 14 kcal/mol.[70] Exceptions to this are the reactions of ethylene with CCH to form vinyl and either acetylene or vinylidene with barriers of 0 and 3 kcal/mol, respectively. These reactions do not contribute significantly in our simulations because CCH is a low coverage, unstable surface intermediate that readily hydrogenates to acetylene under these conditions. The reactions of ethylene with ethylidene to form vinyl and ethyl, and with ethyl to form vinyl and ethane have intrinsic activation barriers of 5 and 2 kcal/mol, respectively, according to our modeling. However, under these conditions with CO, the coverages of ethylene, ethylidene, and ethyl are low.

Thermal Runaway. A major complication in the selective hydrogenation of acetylene in an ethylene rich flow is the onset of thermal runaway.[2] Thermal runaway is the rapid increase of reactor temperature, which causes a degradation in selectivity, rapid increase in ethane production, and the further heating of the reactor. The reactor must be shut down to stop thermal runaway; therefore, the prevention of thermal runaway could potentially reduce the operating costs of the ARU.

The phenomenon of thermal runaway is associated with the loss of selectivity and excess production of ethane. Since ethane is produced predominately from the hydrogenation of ethylene,[3] increased ethane production indicates the onset of rapid ethylene hydrogenation. As noted earlier, it is the ethane production versus temperature, which we determined from our set of isothermal kinetic simulations, that we monitored for the signature of thermal runaway. Figure 3 is a plot of the rate of ethane evolution from the Pd/Ag alloy catalyst with CO present in the feed gas as obtained from our kinetic simulations. The modeling predicts that the rate of ethane production starts to rise at around 450 K and the production increases rapidly up to 550 K. For the pure Pd catalyst in the absence of CO, the entire curve is shifted to lower temperatures by almost 100 K. We attribute the loss of selectivity, rapid ethylene hydrogenation, and the onset of thermal runaway to the increase in the rate of molecular hydrogen dissociation and increase in atomic hydrogen coverage shown in Figure 2. The resultant increase in atomic hydrogen coverage boosts the rates of the nonselective hydrogenation reactions involving atomic hydrogen as the hydrogen source. Figure 4 is a comparison of the atomic hydrogen coverages on the Pd and Pd/Ag catalysts as a function of temperature. The tendency for the alloy catalyst to maintain lower atomic hydrogen coverages makes it less sensitive to thermal runaway.

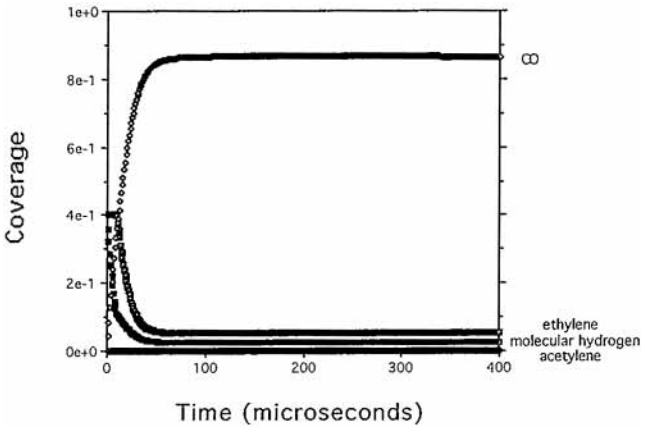

Figure 5. Coverages of CO, H_2, acetylene, and ethylene as a function of time beginning with a clean Pd surface. Reactions between adsorbates are allowed.

The Role of Coadsorbed CO. The manufacture of ethylene through the cracking of hydrocarbons produces small amounts of carbon monoxide.[2] The concentration of the carbon monoxide in the product stream varies according to the operating conditions and feedstock for the cracker. A typical product stream contains approximately 250 ppm of carbon monoxide. Since the front-end ARU does not fractionate the cracker product stream, the reactant stream of the ARU also contains carbon monoxide.[1] At first glance one would think that a species in such low concentration would have little effect on the hydrogenation of acetylene. However, carbon monoxide has been shown to greatly reduce the oligomer formation and decrease the hydrogenation of ethylene.[3,13,14,16,18−20,38,53,81]

Although other binding sites are possible, carbon monoxide, hydrogen, ethylene, and acetylene are usually thought of as being bound in (or near) the bridge site on the palladium surface.[7,13,14,16,28,38,51,78,82−87] Therefore, there is a competition between these four molecules for the space on the surface. The heats of adsorption of each molecule on the catalyst surface is shown in Table 3. Carbon monoxide is the most strongly bound species. Since it is more strongly bound than acetylene by 14 kcal/mol, which is the second most strongly bound of these species, the simulations predict that the surface becomes coated with carbon monoxide, even with the feed gas concentration as low as 250 ppm. Figure 5 shows the results of a kinetic simulation at constant temperature. Carbon monoxide quickly coats 84% of the catalyst surface. The ethylene and hydrogen concentrations drop off dramatically. In the absence of CO, ethylene is the most abundant component under industrial-like conditions, even though it is not the most strongly bound. In this case the most strongly bound component is acetylene, but it is also the most reactive which results in it being relatively scarce as a surface component.

Our estimate for the barrier for acetylene displacement of surface CO from the interior of an island of CO is about 7 kcal/mol. However, the case of ethylene is more severe because the structure of ethylene requires that it displace more than a single surface CO in order to adsorb. Molecular hydrogen is too weakly bound to effectively displace CO (our estimate for this barrier is greater than 25 kcal/mol). The conclusion from our modeling

is that the increase in catalyst selectivity with CO in the feed gas is due to the fact that CO suppresses all other surface species and acetylene is the only component that can displace CO to any significant extent under these conditions. Therefore, the blanket of CO that covers the surface acts like a filter, allowing some acetylene and very little hydrogen and ethylene. This results in significantly higher selectivity and much lower atomic hydrogen coverage by suppressing H_2 adsorption and, indirectly, its dissociation. As mentioned above, the high reactivity of acetylene with H_2 is responsible for the fact that it does not last long on the surface and therefore has a low steady state coverage.

The Effects of Alloying the Pd with Ag. There have been numerous studies of the effects of alloying the palladium catalyst with other metals such as Zn,[88−91] Pb,[88−91] Ag,[42,92−99] Cu,[21−23] Au,[100,101] Ga,[92] In,[92] W,[102] Ni,[103] Mn,[104] La,[105] Sn,[53] Co,[102] and Cr.[106] The palladium−silver alloy catalyst is used commercially.[93−99,107] To better understand the effects of alloying the catalyst, kinetic simulations were performed on an alloy of Pd and Ag for which the ratio of Pd to Ag on the surface is 2:1. This approximates the commercially available palladium−silver alloy catalyst, which consists of an alumina support with silver and palladium deposited on the catalyst in a ratio between 10:1 and 2:1.[93−99,107] The silver is deposited throughout the pellet and the palladium is deposited in a thin layer on the external surface of the catalyst.[107] This deposition method produces a catalyst with a working surface composed of primarily palladium and secondarily silver.

The alloying of the palladium catalyst with silver has similar and complementary effects to the addition of carbon monoxide to the ARU feedstock. Namely the alloy catalyst has a decreased rate of acetylene consumption, increased selectivity, and a greater suppression of thermal runaway than the unimetallic catalyst. Alloying the catalyst with silver decreases the heats of adsorption of all species on the surface by about 1 kcal/mol (Table 3). This decrease in desorption barrier has the effect of increasing the rate of ethylene desorption with respect to ethylene hydrogenation. Therefore, the selectivity of the catalyst increases. Alloying the catalyst with silver increases the hydrogenation barriers from 2 to 4 kcal/mol and from 7 to 9 kcal/mol for acetylene and ethylene, respectively. This shifts the ethylene hydrogenation barrier closer to the ethylene desorption barrier and allows ethylene desorption to compete more favorably with hydrogenation. These factors result in an overall increase in selectivity for acetylene hydrogenation.

Alloying the catalyst with silver increases the dissociation barrier of molecular hydrogen on the surface from 12 kcal/mol to 14 kcal/mol. This effectively decreases the coverage of atomic hydrogen by slowing the rate of dissociation of molecular hydrogen. This is another reason that the Pd/Ag alloy is less sensitive to thermal runaway.

Conclusions

We applied our UBI-QEP and NBI−RPF methods in the modeling of the kinetics of acetylene hydrogenation in an ethylene rich flow over palladium and palladium−silver alloy. Our modeling indicates (1) an acetylene hydrogenation mechanism having atomic hydrogen dominates at low overall coverages, (2) an acetylene hydrogenation mechanism having molecular hydrogenation dominates at high overall coverages, (3) the primary influence on selectivity for acetylene hydrogenation from coadsorption of CO is the suppression of atomic hydrogen on the surface, (4) thermal runaway (runaway ethane production) occurs under conditions favoring higher atomic hydrogen coverages, (5) the high reactivity of acetylene with molecular hydrogen, the relatively slow rate of dissociation of molecular hydrogen, and effects of higher overall coverage (including CO) are the primary factors giving rise to the selective hydrogenation of acetylene, (6) alloying the Pd catalyst with Ag increases selectivity by retarding the molecular hydrogen dissociation and lowering the desorption barrier of ethylene so that ethylene desorption more effectively competes with ethylene hydrogenation, (7) the surface carbonaceous layer does not make a significant contribution as a hydrogen source to the mechanism of hydrogenation under the conditions of our kinetic simulations, (8) oligomer formation on the surface is diffusion controlled, and (9) the relative rates of oligomerization versus hydrogenation of vinyl are controlled by the high rate of hydrogen diffusion and the lower rate of vinyl diffusion. Simulations suggest that oligomer formation is predominately due to reactions involving vinyl, where the vinyl radicals are mainly derived from acetylene. Carbon monoxide suppresses oligomer formation by separating the vinyl radicals on the surface and decreasing their rate of diffusion.

Acknowledgment. We thank the National Science Foundation for the South Dakota EPSCoR Grant (NSF Grant No. EHR-9108773) and Chemical Process Modeling, Inc. for financial support of this work.

References and Notes

(1) Collins, B. M. US patent 4,126,645, 1978.
(2) Bos, A. N. R.; Westerterp, K. R. *Chem. Eng. Proc.* **1993**, *32*, 1.
(3) McGown, W. T.; Kemball, C.; Whan, D. A.; Surrel, M. S. *J. Chem. Soc., Faraday Trans. 1* **1977**, *73*, 632.
(4) Zaera, F. *J. Phys. Chem.* **1990**, *94*, 5090.
(5) Zaera, F.; Somorjai, G. A. *J. Am. Chem. Soc.* **1984**, *106*, 2288.
(6) Kesmodel, L. L.; Dubois, L. H.; Somorjai, G. A. *Chem. Phys. Lett.* **1978**, *56*, 267.
(7) Kesmodel, L. L.; Dubois, L. H.; Somorjai, G. A. *J. Chem. Phys.* **1979**, *70*, 2180.
(8) Kesmodel, L. L.; Gates, J. A. *Surf. Sci.* **1981**, *111*, L747.
(9) Kesmodel, L. L.; Wooddill, G. D.; Gates, J. A. *Surf. Sci.* **1984**, *138*, 464.
(10) Ibach, H.; Hopster, H.; Sexton, B. *Appl. Surf. Sci.* **1977**, *1*, 1.
(11) Ibach, H.; Lehwald, S. *J. Vac. Sci. Technol.* **1978**, *15*, 407.
(12) Deeming, A. J.; Underhill, M. *J. Chem. Soc., Dalton Trans.* **1974**, 1415.
(13) Park, Y. H.; Price, G. L. *Ind. Eng. Chem. Res.* **1991**, *30*, 1693.
(14) Park, Y. H.; Price, G. L. *Ind. Eng. Chem. Res.* **1991**, *30*, 1700.
(15) Park, Y. H.; Price, G. L. *Ind. Eng. Chem. Res.* **1992**, *31*, 469.
(16) McGown, W. T.; Kemball, C.; Whan, D. A. *J. Catal.* **1978**, *51*, 173.
(17) Al-Ammar, A. S.; Thompson, S. J.; Webb, G. *J. Chem. Soc., Chem. Commun.* **1977**, 323.
(18) Al-Ammar, A. S.; Webb, G. *J. Chem. Soc., Faraday Trans 1* **1978**, *74*, 195.
(19) Al-Ammar, A. S.; Webb, G. *J. Chem. Soc., Faraday Trans 1* **1978**, *74*, 657.
(20) Al-Ammar, A. S.; Webb, G. *J. Chem. Soc., Faraday Trans 1* **1979**, *75*, 1900.
(21) Weiss, A. H.; Leviness, S.; Nair, V.; Guczi, L.; Sarkany, A.; Schay, Z. In *Proceedings of the 8th International Congress on Catalysis*; Verlag Chemie: Weinheim, 1984; p 541.
(22) Leviness, S.; Nair, V.; Weiss, A. H.; Schay, Z.; Guczi, L. *J. Mol. Catal.* **1984**, *25*, 131.
(23) Schay, Z.; Sarkany, A.; Guczi, L.; Weiss, A. H.; Nair, V. *Proceedings of the Fifth International Symposium on Heterogeneous Catalysis*; Elsevier: New York, 1983.
(24) Tysoe, W. T.; Nyberg, G. L.; Lambert, R. M. *Surf. Sci.* **1983**, *135*, 128.
(25) Tysoe, W. T.; Nyberg, G. L.; Lambert, R. M. *J. Chem. Soc., Chem. Commun.* **1983**, 623.
(26) Tysoe, W. T.; Nyberg, G. L.; Lambert, R. M. *J. Phys. Chem.* **1984**, *88*, 1960.
(27) Tysoe, W. T.; Nyberg, G. L.; Lambert, R. M. *J. Phys. Chem.* **1986**, *90*, 3188.
(28) Sheridan, J. *J. Chem. Soc.* **1945**, 133.
(29) Beebe, T. P.; Albert, M. R.; Yates, J. T. *J. Catal.* **1985**, *96*, 1.

(30) Beebe, T. P.; Yates, J. T. *J. Am. Chem. Soc.* **1986**, *108*, 663.
(31) Gates, J. A.; Kesmodel, L. L. *Surf. Sci.* **1983**, *124*, 68.
(32) Thomson, S. J.; Webb, G. *J. Chem. Soc., Chem. Commun.* **1976**, 526.
(33) Morrow, B. A.; Sheppard, N. *J. Phys. Chem.* **1966**, *70*, 2406.
(34) Morrow, B. A.; Sheppard, N. *Proc. R. Soc. Ser. A* **1969**, *311*, 391.
(35) Jenkins, G. I.; Rideal, E. K. *J. Chem. Soc.* **1955**, 2490.
(36) Jenkins, G. I.; Rideal, E. K. *J. Chem. Soc.* **1955**, 2496.
(37) Whalley, L.; Davis, B. J.; Moss, R. L. *Trans. Faraday Soc.* **1970**, *66*, 3143.
(38) Moses, J. M.; Weiss, A. H.; Matusek, K.; Guczi, L. *J. Catal.* **1984**, *86*, 417.
(39) Guczi, L.; LaPierre, R. B.; Weiss, A. H.; Biron, E. *J. Catal.* **1979**, *60*, 83.
(40) Margitfalvi, J.; Guczi, L.; Weiss, A. H. *React. Kinet. Catal. Lett.* **1980**, *15*, 475.
(41) Margitfalvi, J.; Guczi, L.; Weiss, A. H. *J. Catal.* **1981**, *72*, 185.
(42) Bond, G. C.; Dowden, D. A.; Mackenzie, N. *Trans. Faraday Soc.* **1958**, *54*, 1537.
(43) Bond, G. C.; Webb, G.; Wells, P. B.; Winterbottom, J. M. *J. Catal.* **1962**, *1*, 74.
(44) Bond, G. C. *Catalysis by Metals*; Academic Press: New York, 1962.
(45) Bond, G. C.; Wells, P. B. *Adv. Catal.* **1964**, *15*, 91.
(46) Bond, G. C.; Wells, P. B. *J. Catal.* **1965**, *4*, 211.
(47) Bond, G. C.; Wells, P. B. *J. Catal.* **1966**, *5*, 419.
(48) Bond, G. C.; Wells, P. B. *J. Catal.* **1966**, *5*, 65.
(49) Bond, G. C.; Webb, G.; Wells, P. B. *Trans. Faraday Soc.* **1965**, *61*, 999.
(50) Bond, G. C.; Webb, G.; Wells, P. B.; Winterbottom, J. M. *J. Chem. Soc.* **1965**, 3218.
(51) King, F.; Jackson, S. D.; Hancock, F. E. *Chem. Ind.* (*Dekker*) **1996**, *68*, 53.
(52) Hancock, F. E.; Booth, J. S. *Proc.-Ethylene Prod. Conf.* **1994**, *3*, 698.
(53) Sarkany, A., Guczi, L.; Weiss, A. H. *Appl. Catal.* **1984**, *10*, 369.
(54) Clotet, A.; Pacchioni, G. *Surf. Sci.* **1996**, *346*, 91.
(55) Asplund, S.; Fornell, C.; Holmgram, A.; Iranloust, S. *Catal. Today* **1995**, *24*, 181.
(56) Derrien, M. L. *Stud. Surf. Sci. Catal.* **1986**, *27*, 613.
(57) Wehrli, J. T.; Thomas, D. J.; Wainwright, M. S.; Trimm, D. L.; Cant, N. W. *Stud. Surf. Sci. Catal.* **1991**, *68*, 203.
(58) Yates, D. J. C.; Lucchesi, P. J. *J. Chem. Phys.* **1961**, *35*, 243.
(59) Inui, T.; Pu, S. B. *Sep. Technol.* **1995**, *5*, 229−237.
(60) Duisenbaev, S. E.; Kharson, M. S.; Beisembaeva, Z. T.; Kiperman, S. L. *Book of Abstracts EuropaCat II Congress, 3−8 September*; MECC: Maastricht, 1995.
(61) Massardier, J.; Bertolini, J. C.; Renouprez, A. in *Int. Congr. Catal. 9th*; 1988; Vol. 3, p 1222.
(62) Haug, K. L.; Burgi, T.; Trautman, T. R.; Ceyer, S. T. *J. Am. Chem. Soc.* **1998**, *120*, 8885.
(63) Azad, S.; Kaltchev, M.; Stacchiola, D.; Wu, G.; Tysoe, W. T. *J. Phys. Chem.* **2000**, *104*, 3107.
(64) Molero, H.; Bartlett, B. F.; Tysoe, W. T. *J. Catal.* **1999**, *181*, 49.
(65) Sellers, H. *J. Chem. Phys.* **1993**, *99*, 650.
(66) Sellers, H. *Surf. Sci.* **1994**, *310*, 281.
(67) Sellers, H. *J. Chem. Phys.* **1994**, *101*, 5201.
(68) Patrito, E. M.; Olivera, Pl Paredes; Sellers, H. *Surf. Sci.* **1994**, *306*, 447.
(69) Gislason, J.; Sellers, H. *Surf. Sci.* **1997**, *385*, 77.
(70) Gislason, J.; Sellers, H. *Surf. Sci.* **1998**, *415*, 70.
(71) Shustorovich, E. *Surf. Sci. Rep.* **1986**, *6*, 1.
(72) Shustorovich, E. *Adv. Catal.* **1990**, *37*, 101.
(73) Shustorovich, E.; Sellers, H. *Surf. Sci. Rep.* **1998**, *242*, 1.
(74) Sellers, H. *Surf. Sci.* **2000**, *459*, 33. (b) Sellers, H.; Gislason, J. *Surf. Sci.* **1999**, *426*, 147.
(75) Brookings Database of metal surface rate constants is maintained by Chemical Process Modeling, Inc. and is a commercially available library of kinetic parameters.
(76) Kash, P. W.; Yang, M. X.; Teplyakov, A. V.; Flynn, G. W.; Bent, B. E. *J. Phys. Chem. B* **1997**, *101*, 7908.
(77) Webb, G. In *Comprehensive Chemical Kinetics*; Bamford, C. H., Tipper, C. F. H., Eds.; Elsevier: Amsterdam, 1978; Vol. 20, p 1.
(78) Reid, J. U.; Thomson, S. J.; Webb, G. *J. Catal.* **1973**, *29*, 433.
(79) Deeming, A. J.; Underhill, M. *J. Chem. Soc., Chem. Commun.* **1973**, 277.
(80) Pradier, C. M.; Mazina, M.; Berthier, Y.; Oudan, J. *J. Mol. Catal.* **1994**, *89*, 211.
(81) Andersen, H. C.; Haley, A. J.; Egbert, W. *Ind. Eng. Chem.* **1960**, *52*, 901.
(82) Ertl, G.; Neumann, M.; Streit, R. *Surf. Sci.* **1977**, *64*, 393.
(83) Krebs, H. J.; Luth, H. *Appl. Phys.* **1977**, *14*, 337.
(84) McCabe, R. W.; Schmidt, L. D. *Surf. Sci.* **1977**, *66*, 101.
(85) Poelsema, B.; Palmer, R. L.; Comsa, G. *Surf. Sci.* **1984**, *136*, 1.
(86) Reid, J. U.; Thomson, S. J.; Webb, G. *J. Catal.* **1973**, *30*, 372.
(87) Reid, J. U.; Thomson, S. J.; Webb, G. *J. Catal.* **1973**, *30*, 378.
(88) Lindlar, H.; Dubuis, R. *Org. Synth.* **1966**, *46*, 89.
(89) Miller, S. A. Academic Press: New York, 1966; Vol. 2, p 1.
(90) Peterson, J. R. Noyes-Data Corp.: Park Ridge, NJ, 1977; p 183.
(91) Palczewska, W. *Chem. Ind.* (*Dekker*) **1988**, *31*, 373.
(92) Sarrazin, P.; Boitiaux, J.-P. Eur. Pat. Appl. EPXXDW.
(93) Johnson, M. M.; Walker, D. W.; Nowack, G. P. U.S. patent 4,-404,124, 1983.
(94) Johnson, M. M.; Walker, D. W.; Nowack, G. P. U.S. patent 4,-484,015, 1984.
(95) Johnson, M. M.; Cheung, T.-T. P. U.S. patent 5,585,318, 1996.
(96) Cheung, T.-T. P.; Johnson, M. M. U.S. patent 5,583,274, 1996.
(97) Cheung, T.-T. P.; Johnson, M. M.; Brown, S. H.; Zisman, S. A.; Kimble, J. B. U.S. patent 5,488,024, 1996.
(98) Cheung, T.-T. P.; Johnson, M. M.; Brown, S. H.; Zisman, S. A.; Kimble, J. B. U.S. patent 5,510,550, 1996.
(99) Brown, S. H.; Zisman, S. A.; Kimble, J. B. U.S. patent 5,587,348, 1996.
(100) Boitiaux, J.-P.; Oosyns, J. U.S. patent 4,533,779, 1985.
(101) Visser, C.; Zuidwijk, J. G. P.; Ponec, V. *J. Catal.* **1974**, *35*, 407.
(102) L'Argentiere, P. C.; Figoli, N. S. *Ind. Eng. Chem. Res.* **1997**, *36*, 2543.
(103) L'Argentiere, P. C.; Canon, M. G.; Figoli, N. S.; Ferrion, J. *Appl. Surf. Sci.* **1993**, *68*, 41.
(104) L'Argentiere, P. C.; Canon, M. G.; Figoli, N. S. *Appl. Surf. Sci.* **1995**, *89*, 63.
(105) L'Argentiere, P. C.; Liprandi, D. A.; Figoli, N. S. *Ind. Eng. Chem. Res.* **1995**, *34*, 3713.
(106) Hudson, H. U.S. patent 4,577,047, 1986.
(107) Shyr, Y.-S. U.S. patent 4,547,486, 1985.